Supporting Information for

A nanoporous metal-organic framework with accessible Cu²⁺ sites for the catalytic Henry reaction

Lian-Xu Shi and Chuan-De Wu*

Department of Chemistry, Zhejiang University, Hangzhou 310027, P. R. China

Email: cdwu@zju.edu.cn

Experimental Section

Materials and General Procedures. All of the chemicals were obtained from commercial sources and were used without further purification, except pyridine-2,3,5,6-tetracarboxylic acid (H₄**pdtc**) and (E)-4-(2-(pyridin-4-yl)vinyl)benzoic acid (H**L**) were synthesized according to the literatures.[1,2] Elementary analysis was performed on a ThermoFinnigan Flash EA 1112 Element Analyzer. IR spectrum was recorded on a KBr pellet with a FTS-40 spectrophotometer. Thermogravimetric analysis (TGA) was carried out under N₂ atmosphere on a NETZSCH STA 409 PC/PG instrument at a heating rate of 10 °C min⁻¹. Powder X-ray diffraction data (PXRD) were recorded on a RIGAKU D/MAX 2550/PC for Cu-Kα (λ = 1.5406 Å). ¹H NMR spectra were recorded on a 500 MHz spectrometer in CDCl₃ solution and the chemical shifts were reported relative to internal standard TMS (0 ppm). The following abbreviations are used to describe peak multiplicity where appropriate: b = broad, s = singlet, d = doublet, t = triplet, q = quartet, m = multiplet. The determinations of the unit cells and data collections for the crystals of compounds **1** and **2** were performed on a *CrysAlisPro* at 293 K. The data sets were corrected by multi-scan absorption correction using spherical harmonics, implemented in SCALE3 ABSPACK scaling algorithm.[3] The structures were solved by direct methods, and refined by full-matrix least-square methods with the **SHELX-97** program package.[4] The solvent molecules in compounds **1** and **2** are highly disordered, and attempts to locate and refine the solvent peaks were unsuccessful. SQUEEZE subroutine of the PLATON software suit was used to remove the scattering from the highly disordered guest molecules. The resulting

new files were used to further refine the structures.[5]

1-(4-nitrophenyl) -2-nitroethanol (a): ^{1}H NMR (500 MHz, CDCl$_3$) δ = 3.25 (s, 1H), 4.56-4.64 (m, 2H), 5.60-5.62 (m, 1H), 7.63 (d, J = 8.7 Hz, 2H), 8.26 (d, J = 8.7 Hz, 2H).

1-(4-nitrophenyl)-2-nitropropan-1-ol (b): (d.r. = 1:2.5) ^{1}H NMR (500 MHz, CDCl$_3$) δ = 1.39 (d, J = 6.9 Hz, 3H), 1.49 (d, J = 6.9 Hz, 1.2H), 3.03 (d, J = 4.3 Hz, 1H), 3.07 (s, 0.4H), 4.75-4.79 (m, 1.4H), 5.2 (dd, J = 4.4, 8.5 Hz, 1H), 5.56 (s, 0.4H), 7.58-7.61 (m, 2.8H), 8.24-8.27 (m, 2.8H).

1-(2-nitrophenyl)-2-nitroethanol (c): ^{1}H NMR (500 MHz, CDCl$_3$) δ = 3.23 (s, 1H), 4.56 (dd, J = 9.1, 13.8 Hz, 1H), 4.87 (dd, J = 2.3, 13.8 Hz, 1H), 6.05 (d, J = 8.9 Hz, 1H), 7.54-7.57 (m, 1H), 7.73-7.76 (m, 1H), 7.96 (d, J = 7.9 Hz, 1H), 8.08 (d, J = 8.3 Hz, 1H).

1-phenyl-2-nitroethanol (d): ^{1}H NMR (500 MHz, CDCl$_3$) δ = 2.97 (d, J = 3.8 Hz, 1H), 4.48 (dd, J = 3.0, 13.3, 1H), 4.58 (dd, J = 9.7, 13.3, 1H), 5.41-5.45 (m, 1H), 7.35-7.41 (m, 5H).

1-(4-bromophenyl)-2-nitroethanol (e): ^{1}H NMR (500 MHz, CDCl$_3$) δ = 2.96 (s, 1H), 4.49 (dd, J =3.0, 13.5 Hz, 1H), 4.57 (dd, J = 9.5, 13.5 Hz, 1H), 5.43 (d, J = 9.3 Hz, 1H), 7.29 (d, J = 8.4 Hz, 2H), 7.53 (d, J = 8.4 Hz, 2H).

References:

1. N. J. Babu, A. Nangia, *Cryst. Growth Des.* 2006, **6**, 1753.

2. H. Kashida, H. Ito, T. Fuji, T. Hayashi, H. Asanuma, *J. Am. Chem. Soc.* 2009, **131**, 9928.

3. Oxford Diffraction Ltd. *CrysAlisPro*, Version 1.171.33.56, **2010**.

4. G. M. Sheldrick, Program for Structure Refinement, University of Göttingen, Germany, **1997**.

5. A. L. Spek, *J. Appl. Crystallogr.* 2003, **36**, 7.

Tables

Table S1. Crystal data and structure refinements for **1** and **2**.

	1	2
Formula	$C_{43}H_{61}Cu_3N_5O_{27}$	$C_{44}H_{32}Cu_3N_6O_{11}$
Formula weight	1270.59	1011.38
Temperature	293(2)	293(2)
Crystal size / mm	$0.32 \times 0.23 \times 0.09$	$0.19 \times 0.18 \times 0.08$
Crystal color	green	blue
Crystal system	triclinic	triclinic
Space group	*P*-1	*P*-1
a (Å)	10.0358(6)	9.9506(7)
b (Å)	15.9728(9)	15.682(2)
c (Å)	21.559(1)	21.500(2)
α (°)	98.333(5)	100.072(9)
β (°)	93.782(5)	93.060(7)
γ (°)	107.759(5)	106.834(8)
Volume ($Å^3$)	3234.1(3)	3142.5(5)
Z	2	2
ρ (g.cm^{-3})	1.305	1.092
$F(000)$	1314	1050
μ (mm^{-1})	1.817	1.612
θ for data collection (°)	2.95 to 67.22	4.72 to 60.06
Limiting indices	$-11 \leq h \leq 11$, $-18 \leq k \leq 18$, $-18 \leq l \leq 25$	$-10 \leq h \leq 11$, $-15 \leq k \leq 17$, $-19 \leq l \leq 23$
Reflection collected	23907 [$R_{int} = 0.0612$]	14772 [$R_{int} = 0.0623$]
Data/parameters	11309 / 523	8960 / 534
Goodness-of fit on F^2	0.959	1.058
R_1 (wR_2) [$I > 2\sigma(I)$]	0.0573 (0.1272)	0.1221 (0.2661)
R_1 (wR_2) (all data)	0.0949 (0.1343)	0.1731 (0.2836)

$R_1 = \sum(| F_o | - | F_c |) / \sum | F_o |$, $wR_2 = [\sum[w(F_o^2 - F_c^2)^2] / \sum w(F_o^2)^2]^{0.5}$.

Table S2. Selected bond lengths (Å) and angles (^{o}) for **1**.

Bond length	(Å)	Bond angle	(^{o})	Bond angle	(^{o})
Cu(1)-N(1)	1.908(3)	N(1)-Cu(1)-N(2)^{i}	177.85(17)	O(10)-Cu(2)-O(3)	99.59(12)
Cu(1)-N(2)^{i}	1.948(3)	N(1)-Cu(1)-O(2)	81.19(13)	O(9)-Cu(2)-O(3)	94.28(13)
Cu(1)-O(2)	2.008(3)	N(2)^{i}-Cu(1)-O(2)	99.46(14)	N(3)^{iii}-Cu(2)-C(23)	129.85(16)
Cu(1)-O(8)	2.021(3)	N(1)-Cu(1)-O(8)	80.20(13)	O(6)^{iv}-Cu(2)-C(23)	127.11(15)
Cu(1)-O(5)^{ii}	2.259(3)	N(2)^{i}-Cu(1)-O(8)	98.82(14)	O(10)-Cu(2)-C(23)	32.21(14)
Cu(2)-N(3)^{iii}	1.950(3)	O(2)-Cu(1)-O(8)	159.19(11)	O(9)-Cu(2)-C(23)	32.57(13)
Cu(2)-O(6)^{iv}	1.984(3)	N(1)-Cu(1)-O(5)^{ii}	96.50(12)	O(3)-Cu(2)-C(23)	96.75(14)
Cu(2)-O(10)	2.026(3)	N(2)^{i}-Cu(1)-O(5)^{ii}	85.48(13)	O(12)-Cu(3)-O(15)	91.74(17)
Cu(2)-O(9)	2.032(3)	O(2)-Cu(1)-O(5)^{ii}	96.55(12)	O(12)-Cu(3)-O(14)	88.75(19)
Cu(2)-O(3)	2.201(3)	O(8)-Cu(1)-O(5)^{ii}	94.72(12)	O(15)-Cu(3)-O(14)	171.8(3)
Cu(2)-C(23)	2.354(4)	N(3)^{iii}-Cu(2)-O(6)^{iv}	101.20(13)	O(12)-Cu(3)-O(4)	170.0(2)
Cu(3)-O(12)	1.927(3)	N(3)^{iii}-Cu(2)-O(10)	160.13(14)	O(15)-Cu(3)-O(4)	85.71(15)
Cu(3)-O(15)	1.963(4)	O(6)^{iv}-Cu(2)-O(10)	95.00(11)	O(14)-Cu(3)-O(4)	92.42(17)
Cu(3)-O(14)	1.986(5)	N(3)^{iii}-Cu(2)-O(9)	97.55(14)	O(12)-Cu(3)-O(13)	98.7(2)
Cu(3)-O(4)	1.983(3)	O(6)^{iv}-Cu(2)-O(9)	158.65(13)	O(15)-Cu(3)-O(13)	95.5(2)
Cu(3)-O(13)	2.366(6)	O(10)-Cu(2)-O(9)	64.71(11)	O(14)-Cu(3)-O(13)	92.5(3)
		N(3)^{iii}-Cu(2)-O(3)	90.22(14)	O(4)-Cu(3)-O(13)	91.08(19)
		O(6)^{iv}-Cu(2)-O(3)	95.77(13)		

Symmetry transformations used to generate equivalent atoms: i) -x+2, -y+2, -z+1; ii) -x+1, -y+1, -z+1; iii) -x-1, -y+1, -z; iv) -x, -y+1, -z+1.

Table S3. Selected bond lengths (Å) and angles (^{o}) for **2**.

Bond length	(Å)	Bond angle	(^{o})	Bond angle	(^{o})
Cu(1)-N(3)^i	1.929(7)	N(3)^i-Cu(1)-O(12)^i	80.9(3)	O(1)-Cu(2)-O(2)	64.5(3)
Cu(1)-O(12)^i	1.981(7)	N(3)^i-Cu(1)-O(6)i	81.3(3)	N(2)-Cu(2)-O(8)^{iii}	90.1(3)
Cu(1)-O(6)^i	1.977(7)	O(12)^i-Cu(1)-O(6)^i	160.1(2)	O(9)^{ii}-Cu(2)-O(8)^{iii}	96.0(3)
Cu(1)-N(1)	1.988(8)	N(3)^i-Cu(1)-N(1)	178.6(4)	O(1)-Cu(2)-O(8)^{iii}	99.5(2)
Cu(1)-O(10)	2.249(7)	O(12)^i-Cu(1)-N(1)	98.3(4)	O(2)-Cu(2)-O(8)^{iii}	94.4(3)
Cu(2)-N(2)	1.979(8)	O(6)^i-Cu(1)-N(1)	99.3(4)	O(4)-Cu(3)-N(4)	86.4(7)
Cu(2)-O(9)^{ii}	2.024(6)	N(3)^i-Cu(1)-O(10)	96.0(3)	O(4)-Cu(3)-O(13)	93.9(6)
Cu(2)-O(1)	2.043(6)	O(12)^i-Cu(1)-O(10)	92.7(2)	N(4)-Cu(3)-O(13)	172.8(5)
Cu(2)-O(2)	2.058(6)	O(6)^i-Cu(1)-O(10)	97.9(3)	O(4)-Cu(3)-O(7)^{iv}	169.5(7)
Cu(2)-O(8)^{iii}	2.162(8)	N(1)-Cu(1)-O(10)	85.1(3)	N(4)-Cu(3)-O(7)^{iv}	93.1(5)
Cu(3)-O(4)	1.892(17)	N(2)-Cu(2)-O(9)^{ii}	100.4(3)	O(13)-Cu(3)-O(7)^{iv}	85.4(4)
Cu(3)-N(4)	1.958(14)	N(2)-Cu(2)-O(1)	160.8(3)	O(4)-Cu(3)-O(15)	96.6(8)
Cu(3)-O(13)	1.967(10)	O(9)ii-Cu(2)-O(1)	95.1(3)	N(4)-Cu(3)-O(15)	96.2(7)
Cu(3)-O(7)^{iv}	2.012(8)	N(2)-Cu(2)-O(2)	98.4(3)	O(13)-Cu(3)-O(15)	90.9(6)
Cu(3)-O(15)	2.253(18)	O(9)^{ii}-Cu(2)-O(2)	158.4(3)	O(7)^{iv}-Cu(3)-O(15)	93.9(6)

Symmetry transformations used to generate equivalent atoms: i) -x-1, -y-2, -z+3; ii) -x+1, -y-1, -z+3; iii) x+1, y+1, z; iv) -x+2, -y-1, -z+4.

Figures:
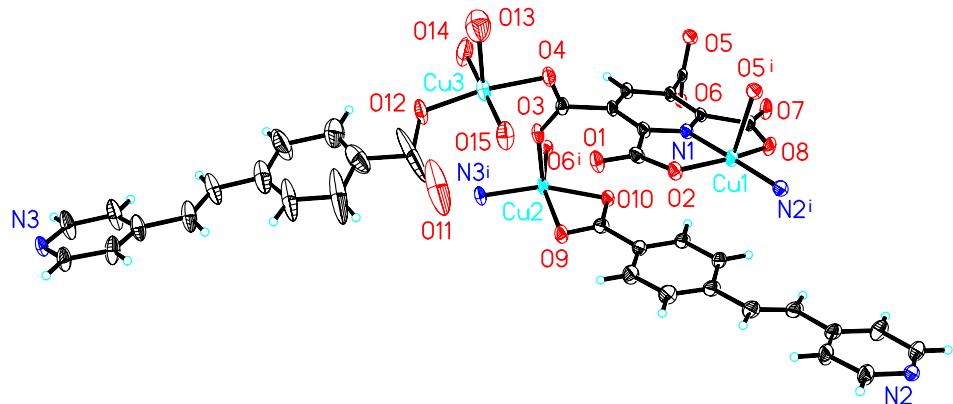
Figure S1. ORTEP representation of the symmetry expanded local structure for **1** (25% probability ellipsoids).
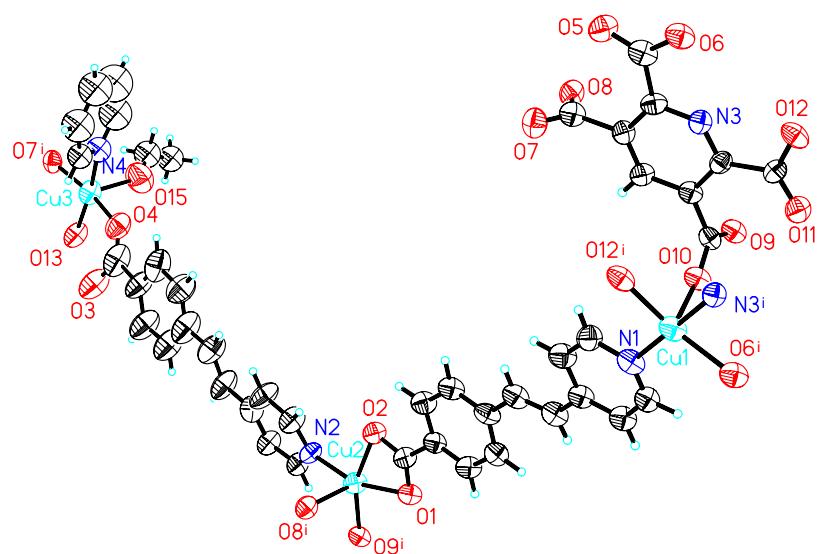
Figure S2. ORTEP representation of the symmetry expanded local structure for **2** (25% probability ellipsoids).
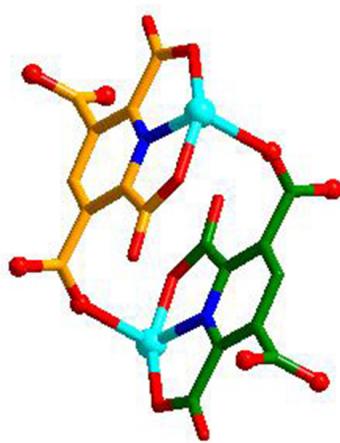
**Figure S3**. A view of the dinuclear unit in **1**.
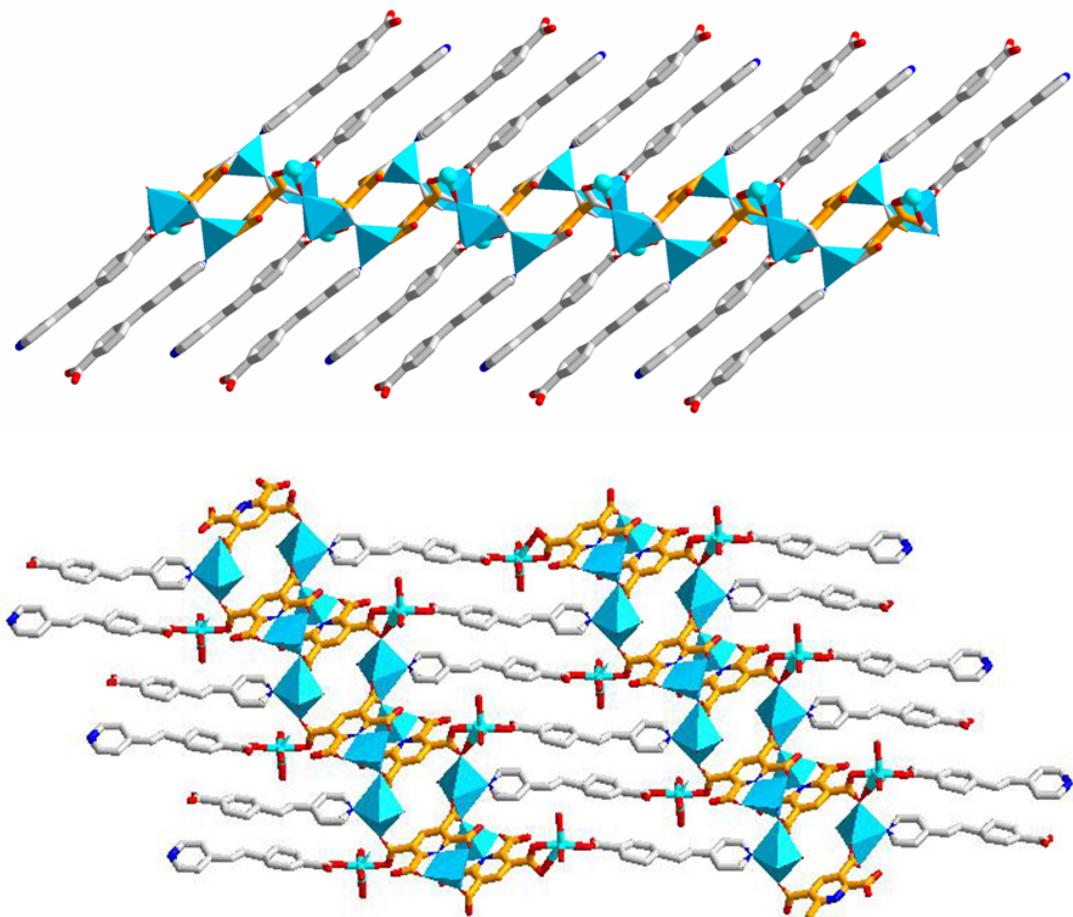
**Figure S4**.   A view of the 1D polymeric subunits linked by two kinds of **L** ligands in

1.
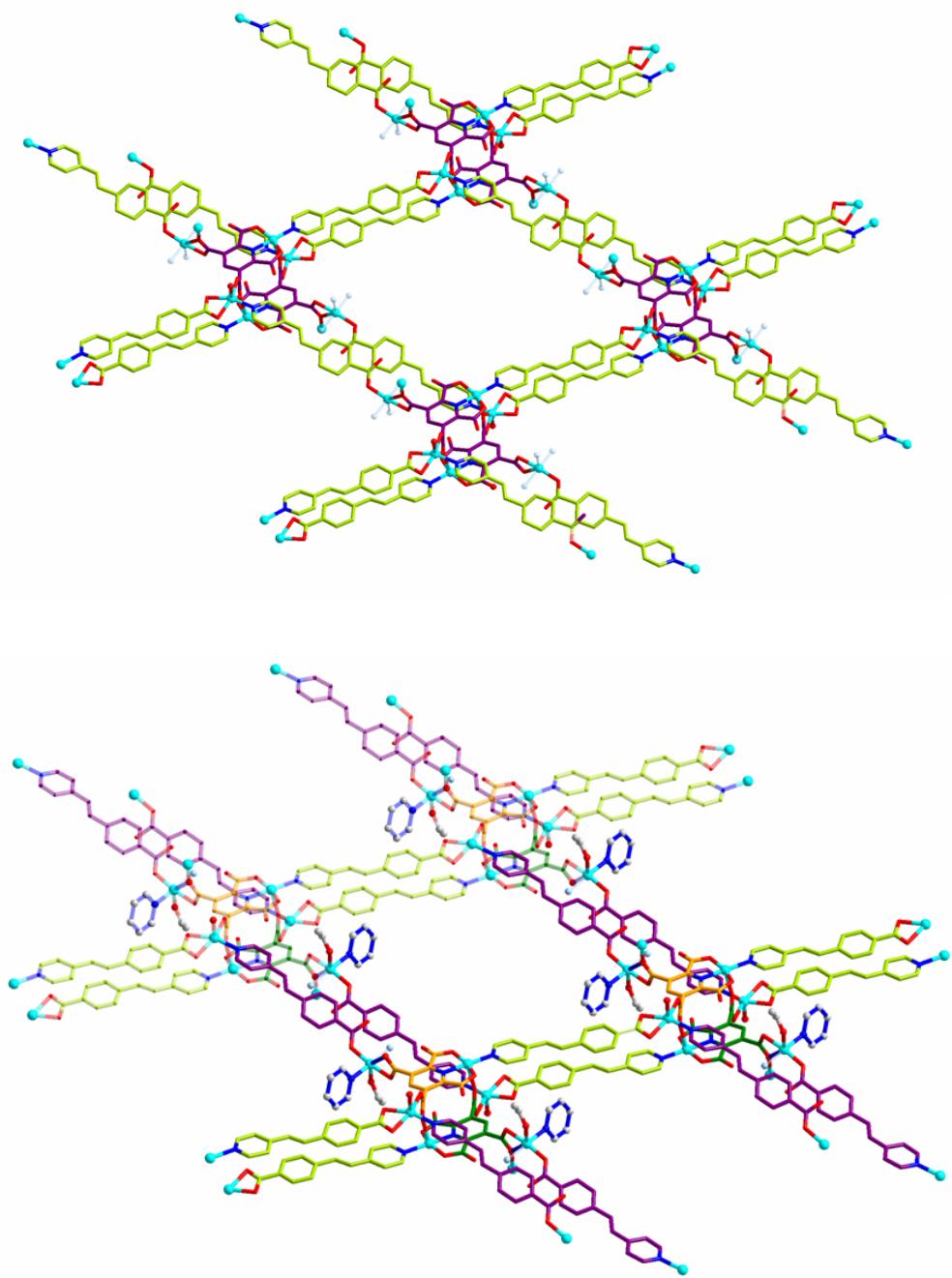
Figure S5. A view of the coordination environments of the active copper atoms before (up) and after (bottom) being immersed in pyridine/EtOH solution.
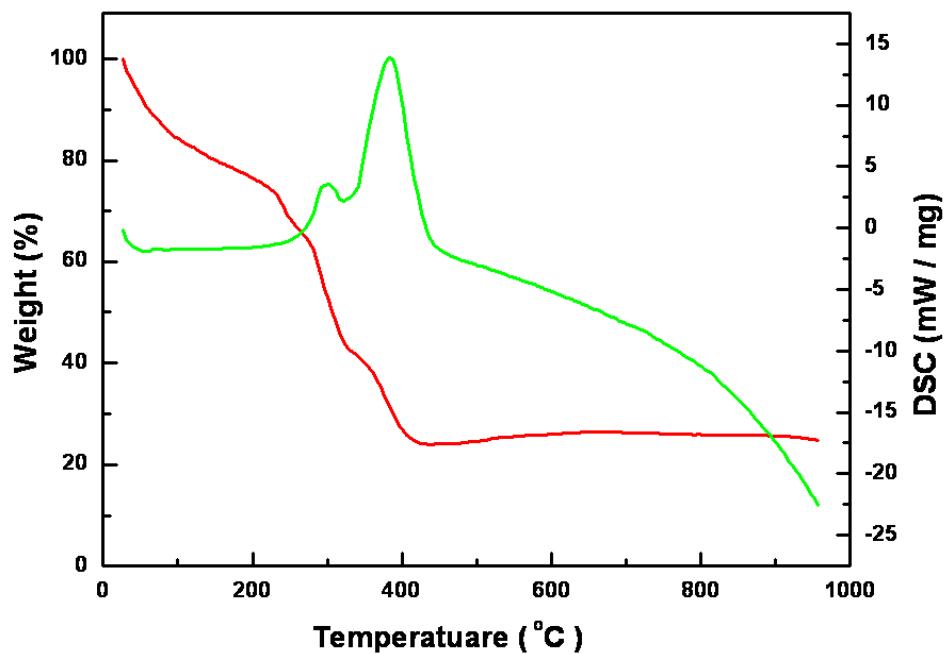
Figure S6. TGA results of **1**.
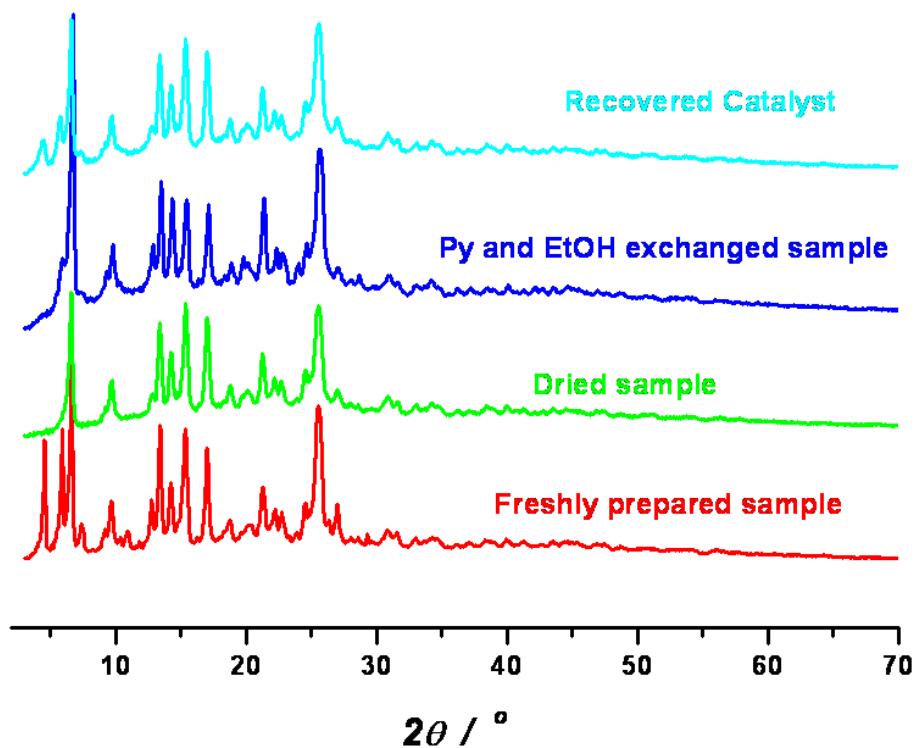
Figure S7. Powder X-ray diffraction patterns for compound **1**.
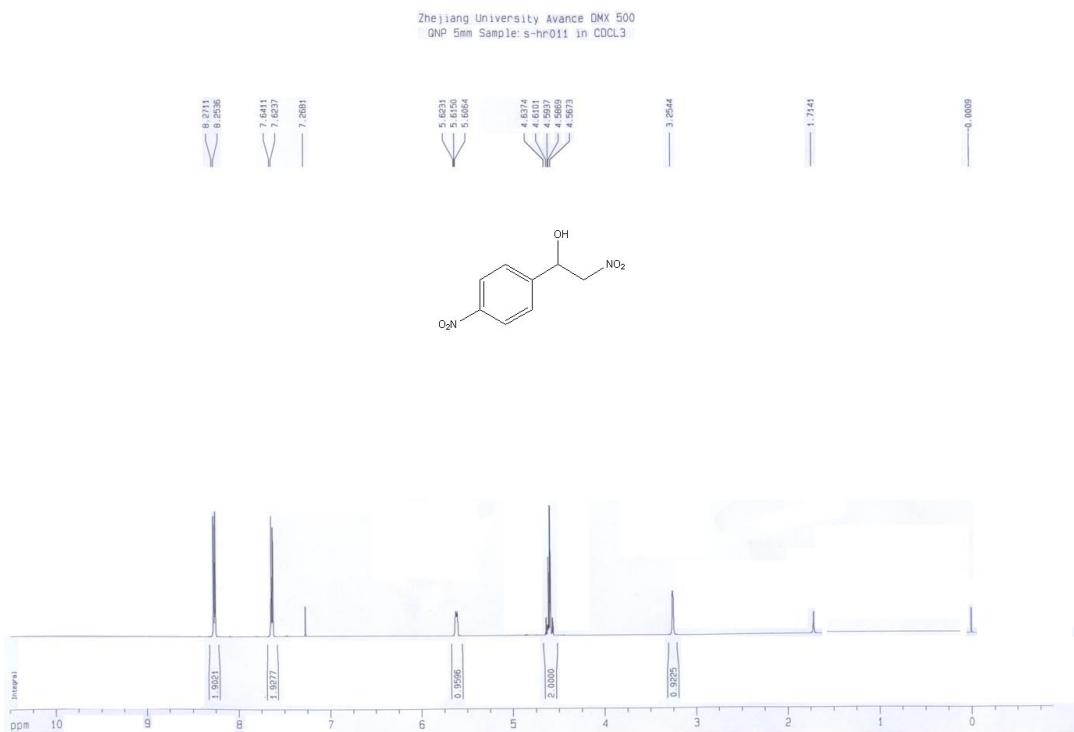
Figure S8. ^{1}HNMR spectrum for **1-(4-nitrophenyl) -2-nitroethanol (a)**.
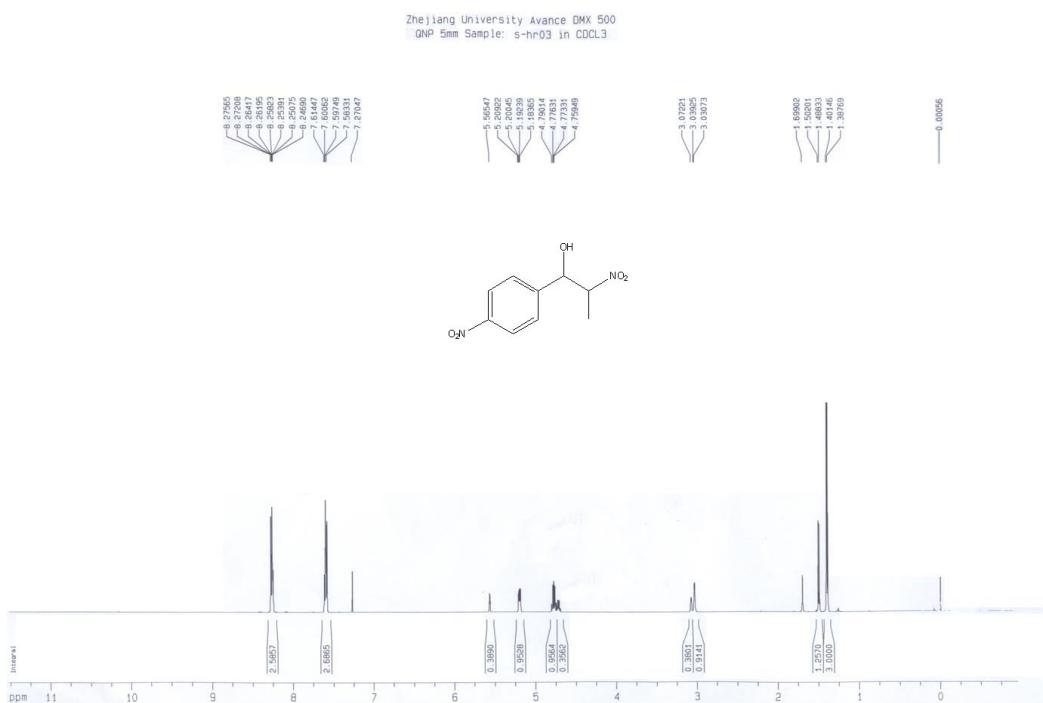
Figure S9. ^{1}HNMR spectrum for **1-(4-nitrophenyl)-2-nitropropan-1-ol (b)**.
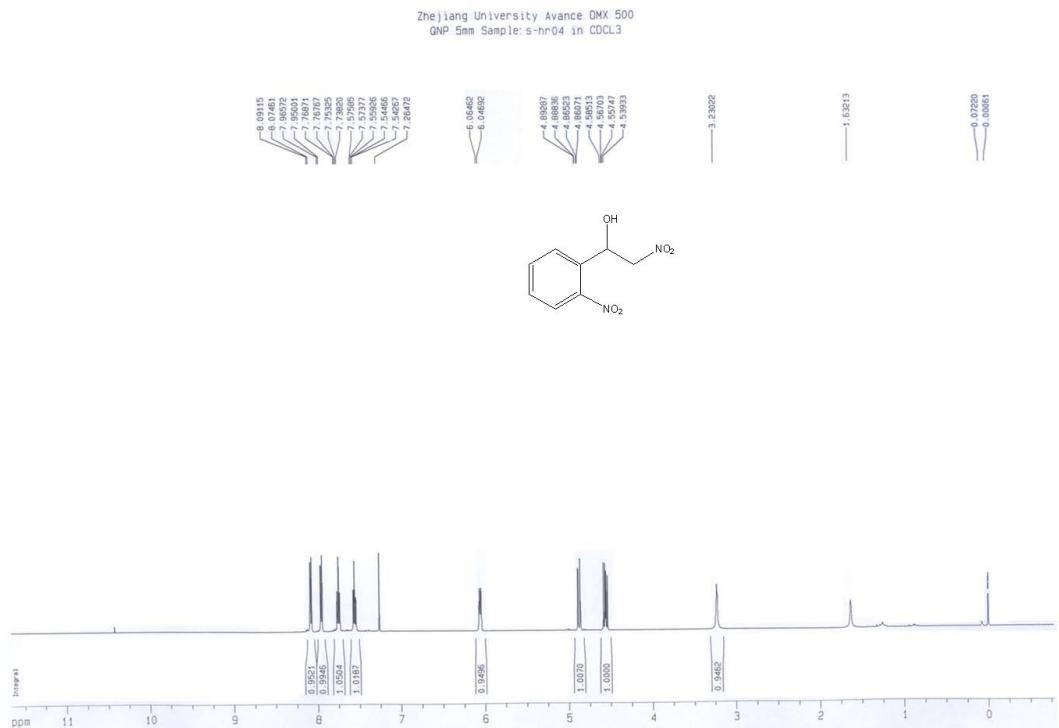
Figure S10. ^{1}HNMR spectrum for **1-(2-nitrophenyl)-2-nitroethanol (c)**.
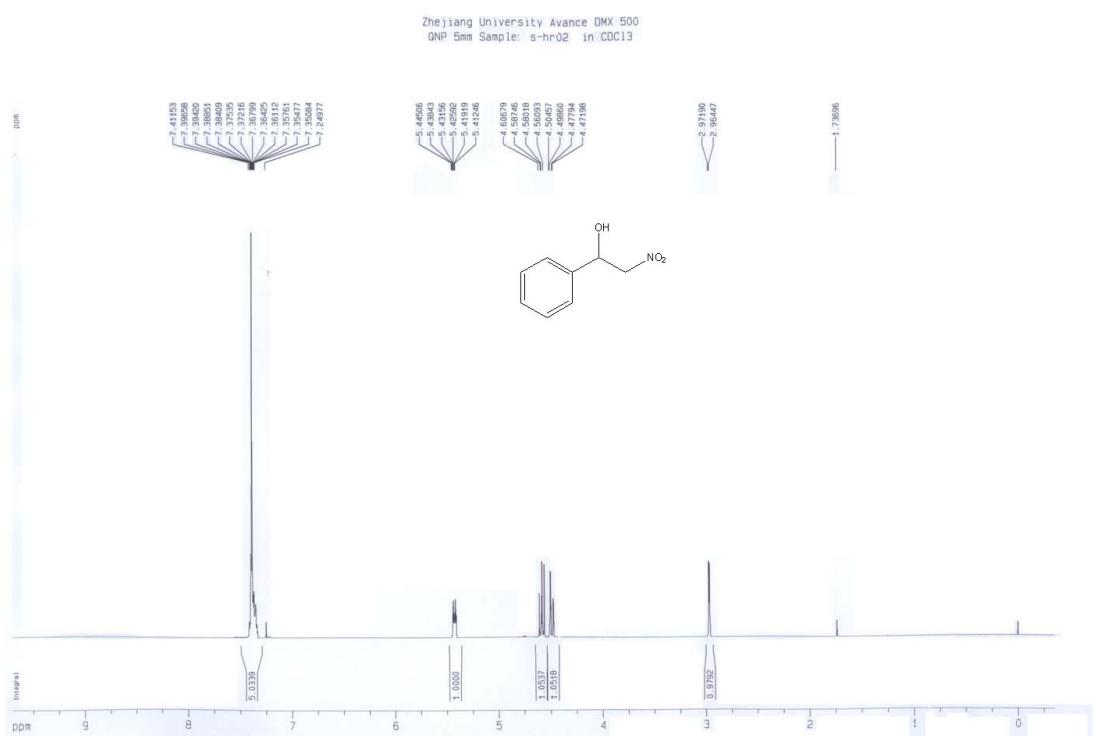
Figure S11. ^{1}HNMR spectrum for **1-phenyl-2-nitroethanol (d)**.
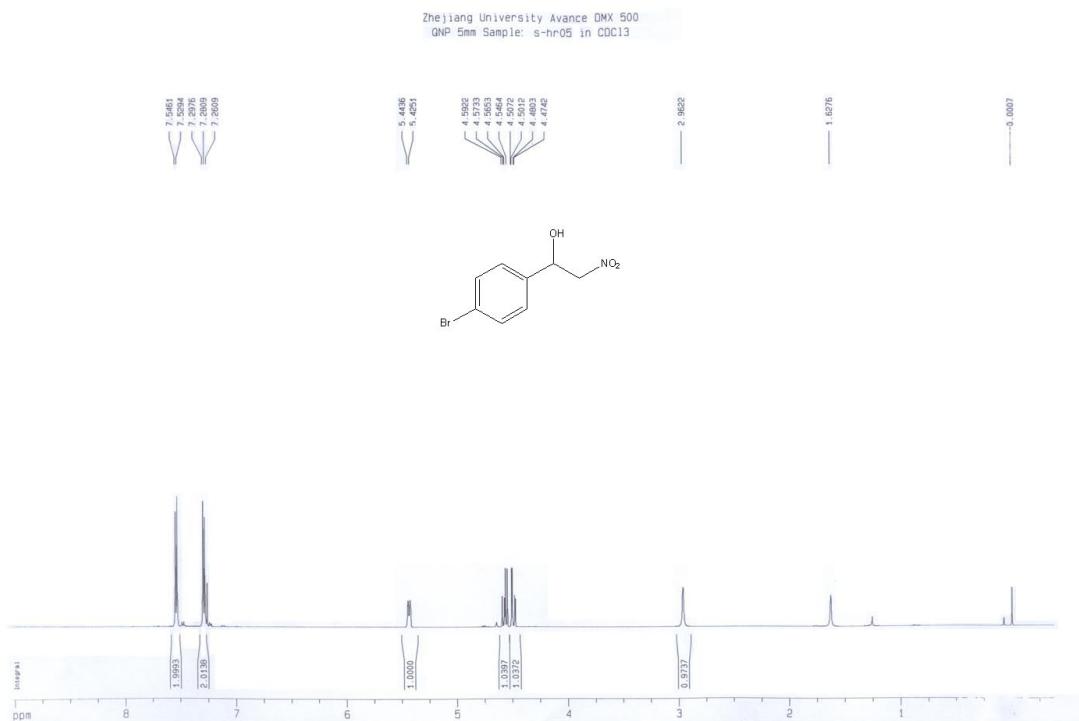
**Figure S12.** ^{1}HNMR spectrum for **1-(4-bromophenyl)-2-nitroethanol (e)**.
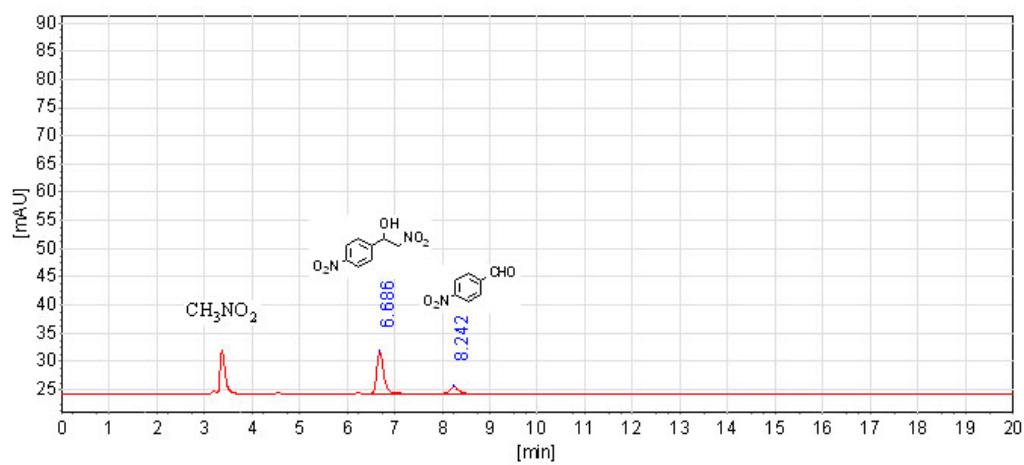
Figure S13. HPLC trace of the Henry reaction of CH_3NO_2 and 4-nitrobenzaldehyde catalyzed by **1** (Table 1, entry 1).
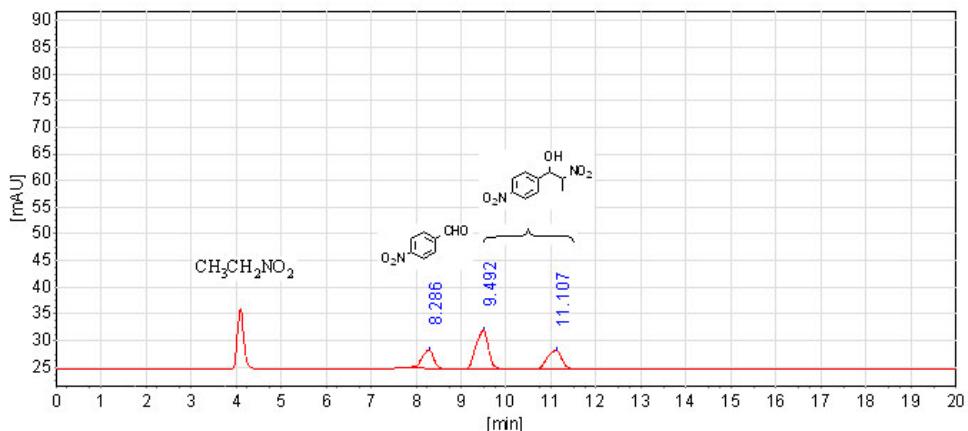
Figure S14. HPLC trace of the Henry reaction of $C_2H_5NO_2$ and 4-nitrobenzaldehyde catalyzed by **1** (Table 1, entry 2).
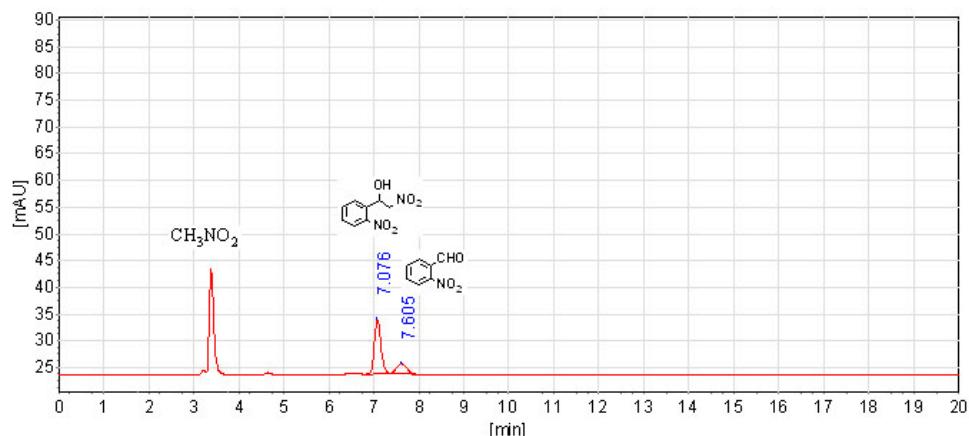
Figure S15. HPLC trace of the Henry reaction of CH_3NO_2 and 2-nitrobenzaldehyde catalyzed by **1** (Table 1, entry 3).
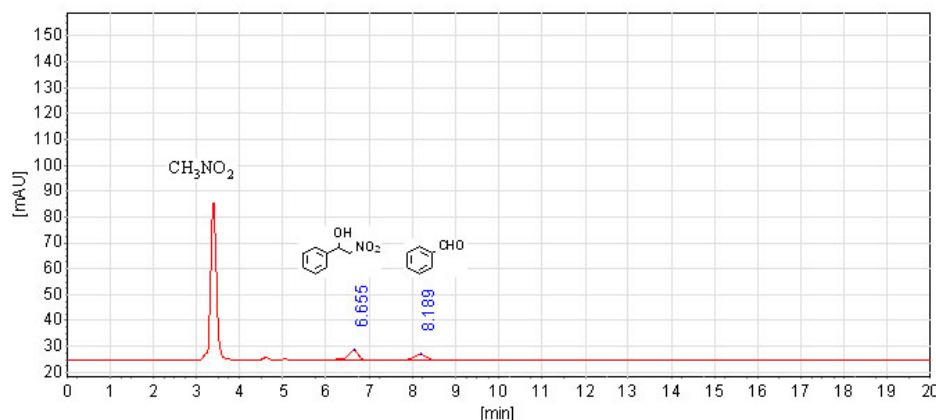

Figure S16. HPLC trace of the Henry reaction of CH_3NO_2 and benzaldehyde catalyzed by **1** (Table 1, entry 4).
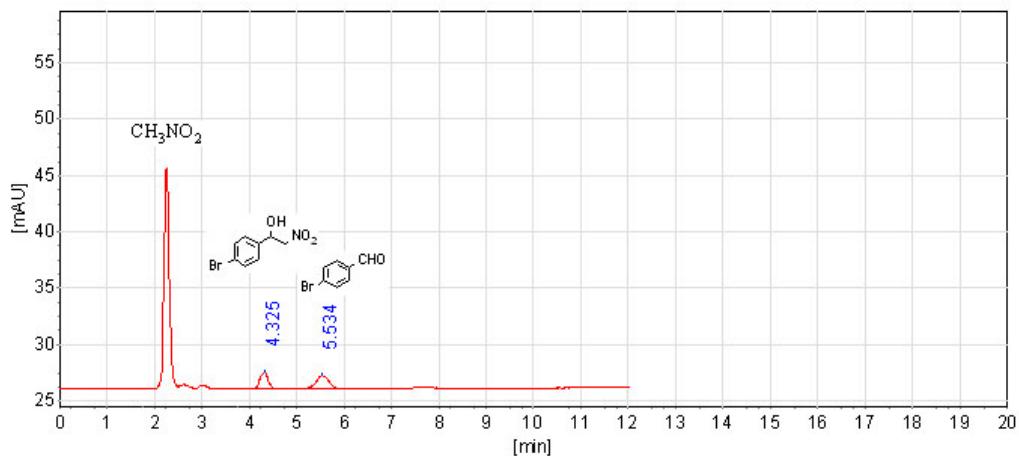
Figure S17. HPLC trace of the Henry reaction of CH_3NO_2 and 4-bromobenzaldehyde catalyzed by **1** (Table 1, entry 5).
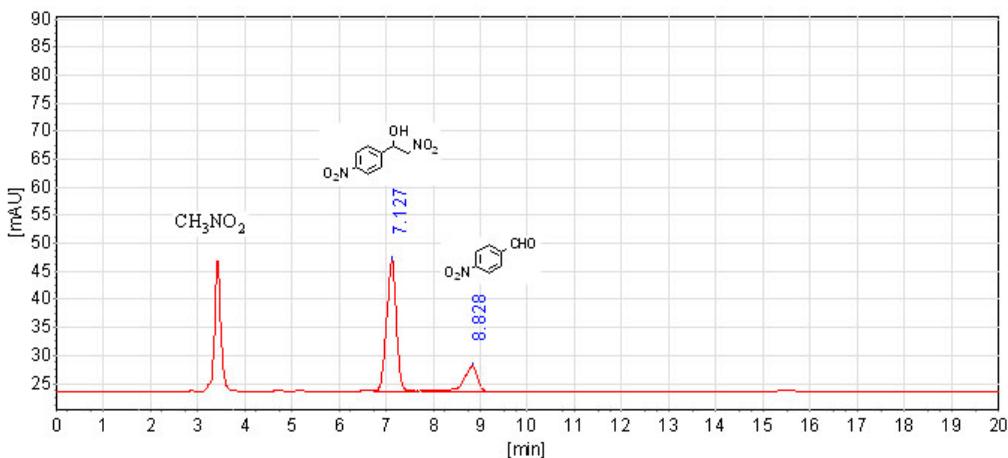

Figure S18. HPLC trace of the Henry reaction of CH_3NO_2 and 4-nitrobenzaldehyde catalyzed by the recovered solid **1** (the fifth cycle; Table 1, entry 9).